Atmos. Chem. Phys. Discuss., 12, 3595–3617, 2012
www.atmos-chem-phys-discuss.net/12/3595/2012/
doi:10.5194/acpd-12-3595-2012

Atmospheric Chemistry and Physics Discussions

Effects of cosmic ray decreases on cloud microphysics

J. Svensmark, M. B. Enghoff, and H. Svensmark

National Space Institute, Technical University of Denmark, Copenhagen, Denmark

Received: 11 November 2011 – Accepted: 16 January 2012 – Published: 1 February 2012

Correspondence to: M. B. Enghoff (enghoff@space.dtu.dk)

Published by Copernicus Publications on behalf of the European Geosciences Union.

Effects of cosmic ray decreases on cloud microphysics

J. Svensmark et al.

Abstract

Using cloud data from MODIS we investigate the response of cloud microphysics to sudden decreases in galactic cosmic radiation – Forbush decreases – and find responses in effective emissivity, cloud fraction, liquid water content, and optical thickness above the 2–3 sigma level 6–9 days after the minimum in atmospheric ionization and less significant responses for effective radius and cloud condensation nuclei (<2 sigma). The magnitude of the signals agree with derived values, based on simple equations for atmospheric parameters. Furthermore principal components analysis gives a total significance of the signal of 3.1 sigma. We also see a correlation between total solar irradiance and strong Forbush decreases but a clear mechanism connecting this to cloud properties is lacking. There is no signal in the UV radiation. The responses of the parameters correlate linearly with the reduction in the cosmic ray ionization. These results support the suggestion that ions play a significant role in the life-cycle of clouds.

1 Introduction

It has been suggested that galactic cosmic rays (GCRs), through ionization, affect the formation of aerosols in the atmosphere, which in turn affects Earth's cloud cover (Dickinson, 1975; Svensmark and Friis-Christensen, 1997; Marsh and Svensmark, 2000; Bagó and Butler, 2000). In evaluating this idea, much attention has recently been directed to the subject of coronal mass ejections and their subsequent depression of the galactic cosmic ray influx as first noticed by Forbush (1937). The duration of these sudden "Forbush decreases" (FDs) in the GCRs appears comparable to the growth times of atmospheric aerosols from nucleation to CCN sizes – typically one day to a week (Kulmala et al., 2004).

Although Svensmark et al. (2009) (SBS) found that the amount of low clouds and aerosol Angstrom exponent showed a significant decrease during FDs, there is an ongoing debate whether an actual effect is detectable or not. Works by Sloan and Wolfendale (2008), Laken et al. (2009), and Calogovic et al. (2010) report that no statistically significant signal is to be found during FDs. Kristjánsson et al. (2008) and Todd and Kniveton (2004) found some response, a study by Rohs et al. (2010) reports a significant signal in high- and mid-level clouds, and Dragić et al. (2011) found a strong signal by using the diurnal temperature range as a cloudiness proxy, allowing them to extend the period of investigation beyond the satellite era. Modelling work by Bondo et al. (2010) suggests that an effect could be observable in the aerosols under atmospheric conditions while extensive modelling results from Snow-Kropla et al. (2011) find very little response. Ions, which are partly created by cosmic rays, have been found to account for 1–30 % of aerosol nucleation at several European measurement sites (Manninen et al., 2010) and this fraction may turn out to be even higher (Yu and Turco, 2011). If indeed there exists a link between cosmic rays, aerosols, and clouds, it is reasonable to expect an actual change in several cloud microphysical parameters on a global scale during an FD, and not just in cloud fraction.

In this study observations from the Moderate Resolution Imaging Spectroradiometer (MODIS) aboard the Terra satellite were used to examine the response in six cloud microphysical parameters during FDs. Beside the liquid water cloud fraction (CF) previously examined by SBS, we include the cloud effective emissivity (ϵ), the column density of the cloud condensation nuclei (CCN), the cloud optical thickness (τ), the liquid water path (LWP), and the liquid cloud effective radius (R_{eff}). The observed variations are then discussed with respect to a mechanism involving changes in GCR flux, Total Solar Irradiance (TSI), or UV light.

2 Data

The 13 strongest FDs in the time period 2000–2006, with regard to ionization changes, were chosen for this analysis and are listed in Table 1. After 2006 no strong FDs occurred due to the prolonged minimum between solar cycles 23 and 24. The FDs are

ACPD
12, 3595–3617, 2012

ordered with a descending impact on ionization rate in the lower atmosphere ($\leq$3 km), such that FD 1 causes a larger ionization decrease than FD 2, and so forth; for further details see Svensmark et al. (2009). Rating of the FDs according to lower atmosphere ionization is important, as this is where cosmic ray intensity and clouds appear to show the strongest correlation (Marsh and Svensmark, 2000). Only the strongest events are used to avoid any dilution of the signal by including weak events.

For each FD, a time interval of 15 days prior to and 20 days after the FD minimum was used, so that the base level of a given parameter, its potential change due to the FD, and its path back to the base level would all be included. The FD minimum is defined as the day with the lowest cosmic ray count rate (day 0).

The data product "MOD08_D3" available from the MODIS website offers a daily average map covering all of the Earth for over 600 geophysical products. The six parameters mentioned in the introduction were chosen because of their significance for the cloud microphysics. Table 2 lists the MODIS parameters used here, together with their corresponding names in the MODIS data set.

To overcome signal and weather induced noise, each daily map was averaged into a global daily mean value $P_i(t)$. Here P indicates the parameter in question and i the index number of the FD in Table 1. The CCN product is based on the derived aerosol size distribution, which is based on an inversion using optical thickness and reflectance data (see Remer et al., 2005, for details). Also note that CCN is only retrieved over the ocean as aerosol counts are difficult to retrieve over land (Levy et al., 2010).

For each parameter one hundred 36 day intervals were made. Each interval had their linear trend removed and was normalised to their standard deviation. The resulting ~3 k days (some had to be removed due to lack of data) were plotted and a chi-squared test was done to see if they fit a normal distribution. In all cases the fits were significant (see the Supplement) and this ensures that statistical tests relying on a normal distribution of the data can be employed.

ACPD
12, 3595–3617, 2012

3 Results

3.1 Forbush decrease means

Global values for the six parameters can be seen in Fig. 1 for the mean of FDs 1 to 5. These events are far stronger than the remaining eight and thus have a better probability to show an effect above the noise – since Fig. 1 shows the temporal evolution of the events it becomes even more important only to include the strongest FDs. Light grey areas indicate the standard deviation (σ) of the data sets, and dark grey areas indicate 2 standard deviations. The standard deviations are calculated from the mean standard deviation of 100 realizations of the mean of 5 randomly placed 36-day intervals, chosen from the 2000–2006 MODIS data, excluding the FD event intervals.

We note that the decreases in ϵ, τ, LWP, and CF extend beyond $2\,\sigma$. τ, LWP, and CF briefly reach their minimum value 6 days after the FD minimum, whereas ϵ reaches its minimum at day 8. R_{eff} reaches a maximum at day 11, but this is below $2\,\sigma$ while CCN shows a minimum at day 9, also below $2\,\sigma$. The extremum days, as the average of the five individual events, are summarized in Table 3, Column 6.

3.2 Forbush decrease magnitudes

To quantify the connection between the magnitude of a Forbush decrease and its response in a given parameter it is necessary to define the percentage change in ionization caused by the FD, and the corresponding percentage change (c_{P_i}) in $P_i(t)$. The percentage FD strength is listed in Table 1 for each FD event, calculated by the SBS method. For all of the parameters and for all of the events in Table 1 c_{P_i} was calculated from the mean of day −15 to −5 (the base level) and the extremum value between day 0 and day 15 of the FD. For R_{eff} we searched for maximum values, for the other five parameters we searched for minimum values.

Plotting the change in $P_i(t)$ as a function of FD strength shows whether or not there exists a systematic connection. A series of such plots for all of the parameters can be

ACPD
12, 3595–3617, 2012
Effects of cosmic ray decreases on cloud microphysics
J. Svensmark et al.

seen in Fig. 2. The outlier on the right of each plot is FD 1, which was unusual as it occured during the 2003 Halloween event along with 11 X-class solar flares in 18 days (Woods et al., 2004). We apply a Student's t-test to test if the slopes are different from zero. The slope of ϵ is significant at the 98 % level (99 % excluding FD 1), CF at 95 % (90 % excluding FD 1), LWP at 95 %, R_{eff} at 95 % excluding FD 1 and insignificant when including it, and τ at the 95 % level (99 % excluding FD 1). The slope of the CCN is significant at the 90 % level when excluding FD 1 and insignificant when including it. In short, a decrease in GCR influx precedes a decrease in ϵ, CF, LWP, and τ and possibly an increase in R_{eff}.

4 Discussion

The ordering of the FD events (Table 1) is of crucial importance to the investigation of their possible influences on cloud cover. Detecting a signal in cloud parameters has proven to be a struggle against noise, and only the most powerful of FDs show an effect in cloud parameters larger than ~2 standard deviations. An analysis of less powerful FDs will therefore be dominated by noise. This may also help to explain why some similar studies did not find any significant signal. For instance Calogovic et al. (2010) examined 6 FDs from the International Satellite Cloud Climate Project (ISCCP) data set, and concluded that there is no effect to be found. None of the FDs used in their analysis are included in the present analysis since they occurred before the launch of MODIS, but they all rank low in the SBS table. Therefore any signal will most likely be obscured by noise. Kristjánsson et al. (2008) examined means of 22 FDs using MODIS. As most of these caused only small ionization changes, the mean signal lies within the meteorological noise, and this may explain why they observed no signal and why their signal improved when they looked at their 6 strongest events (which rank high on the SBS list too). Sloan and Wolfendale (2008) focused in part on monthly averaged data from ISCCP. As the present study along with the SBS paper shows, the effect peaks about a week after the FD minimum; monthly averages are unlikely to show a signal.

ACPD
12, 3595–3617, 2012

Laken et al. (2009) suggested that the signals in the SBS paper are caused by random fluctuations but provided no strong statistical foundation for their conclusion. In light of these observations we build our analysis on strict statistical arguments to go along with the physical explanations.

4.1 Derived changes

Columns 2 and 3 of Table 3 lists the mean base levels and their mean percentage changes for the 5 largest events as obtained by methods discussed in the previous sections. To evaluate if these changes in each individual parameter are reasonable with respect to the changes in other parameters, the following equations can be used (Stephens, 1978) (Eq. 1) and (Hobbs, 1993, Chap. 2) (Eqs. 2–3):

$$\epsilon = 1 - e^{-a_0 \mathrm{LWP}} \tag{1}$$

$$\tau \approx \frac{3}{2\rho} \frac{\mathrm{LWP}}{R_{\mathrm{eff}}} \tag{2}$$

$$\tau \approx 2.4 \left(\frac{\mathrm{LWP}}{\rho} \right)^{2/3} (N_{\mathrm{c}})^{1/3} \tag{3}$$

Here ρ is the density of water ($1000\,\mathrm{kg\,m^{-3}}$), a_0 is a scaling parameter (found by using base levels for LWP and ϵ in the MODIS data and solving for a_0), and N_{c} is the droplet column density and will be approximated as CCN.

The derived percentage changes for each parameter ($c_{P_{1..5,\mathrm{der}}}$) are found by inserting the base levels (from Table 3) of any of the other parameters they depend on along with the changes in these parameters during an FD, e.g. for τ:

$$\tau_a = \frac{3}{2\rho} \frac{\mathrm{LWP}}{R_{\mathrm{eff}}} \tag{4}$$

$$\tau_b = \frac{3}{2\rho} \frac{\mathrm{LWP} + \Delta \mathrm{LWP}}{R_{\mathrm{eff}} + \Delta R_{\mathrm{eff}}} \tag{5}$$

Discussion Paper | Discussion Paper | Discussion Paper | Discussion Paper |

ACPD

12, 3595–3617, 2012

Effects of cosmic ray decreases on cloud microphysics

J. Svensmark et al.

$$c_{\tau_{1..5,\mathrm{der}}} = \frac{\tau_b - \tau_a}{\tau_a} \times 100\% = -3.73 \pm 1.54\%. \tag{6}$$

Table 3 lists the derived parametric changes and the measured percentage drop of $-2.87\,\%$ in τ lies well within the uncertainty of the derived value.

Using the same approach to Eq. (3) for N_c, the derived change is $c_{N_{\mathrm{c}_{1..5,\mathrm{der}}}} = -2.49 \pm 5.32\,\%$. Assuming that CCN changes as N_c, the derived signal for CCN is thus within one standard deviation of the CCN data shown in Fig. 1. This is consistent with the lack of a significant signal for CCN either in Figs. 1 or 2. The derived value for R_eff also lies within the noise. Inserting the values for ϵ, LWP, and τ in Eqs. (1–3), the derived parametric changes ($c_{P_{1..5,\mathrm{der}}}$) are consistent with the observations ($c_{P_{1..5,\mathrm{meas}}}$), regardless of which equation was used to find the derived values for those parameters that appear in more than one equation – the results are summarized in Table 3.

4.2 Principal components analysis

To further test the significance of the results a principal components analysis was performed on the six parameters. This gives a measure of the total disturbance of the cloud microphysics during the FD events. For the top five events each parameter was normalized by subtracting its mean value, removing the linear trend, and dividing by the standard deviation of the entire time interval. Eigenvalues and principal components (PCs) were then found from the resulting correlation matrix. Figure 3 shows the time series along the first PC from day −60 to 60. The uncertainty was determined by generating the PC from day −100 to day 0 and take the standard deviation. A clear, broad signal of 3.1 is apparent and shows that the signal in the microphysical parametric system is simultaneous in all (or most) parameters and statistically significant even when the timespan is expanded far beyond the event. Regardless of the interval used the signal remains robust: $2.8\,\sigma$ for day −15–20, $2.8\,\sigma$ for day −40–40, $3.3\,\sigma$ for day −80–80, and $2.9\,\sigma$ for day −100–100. For these extended time series there were periods with missing data, which were set to 0 (only for the event(s) with missing data) after

ACPD
12, 3595–3617, 2012

Effects of cosmic ray decreases on cloud microphysics

J. Svensmark et al.

removal of the linear trend. The same was done with a few extreme outliers connected with the periods of missing data.

The eigenvalues of the correlation matrix may also be used as a measure of the amount of variance in a multivariable time series (Miller and Miller, 2000, Chap. 8). For non-FD data the first eigenvalue is 2.3 (2.0 when filtered for periods of over 90 days). When all FD-events are arranged as a continuing time series (36 days for each), without removing any linear trend, the first eigenvalue increases to 3.1, and for the 5 strongest events it becomes 3.8. Removing day −15 to 0 from each FD increases it further to 4.0 (for the five strongest events, 3.2 for all thirteen events). The total variance of the system is 6 (1 for each parameter) so this could be interpreted as PC1 containing the signal from the four parameters that show a response above 2 standard deviations. This further supports the conclusion that actual disturbances of the cloud system occur during FD events.

4.3 Intercorrelation

Intercorrelation between the investigated parameters is another potential issue. One reason for this could be if some of the parameters are measured with the same optical channels or are used to derive each other. King et al. (1997, Table 1) shows that optical thickness and effective radius use different wave bands but, for instance, the liquid water path is derived from the optical thickness and effective radius (King et al., 1997, page 65). In Fig. 4 we look at the intercorrelation between the used parameters. Of the correlations shown, the highest ($r = 0.88$) is between optical thickness and liquid water path, which is not surprising given their shared origin. Otherwise cloud fraction and emmisivity are the only other pair with an r value above 0.5.

4.4 UV and TSI

A change in UV could be important for aerosol formation and therefore for cloud microphysics. We examined how the signal in UV and TSI correlates with FDs, similarly to how it was done with the cloud microphysical parameters in Figs. 1 and 2. Data

ACPD
12, 3595–3617, 2012

Effects of cosmic ray decreases on cloud microphysics

J. Svensmark et al.

was obtained from NOAA's MgII Core-to-wing ratio (UV) (Viereck and Puga, 1999) and the VIRGO Experiment on the cooperative ESA/NASA Mission SOHO (TSI) (Froehlich, 2006). Figure 5 shows how TSI and UV vary following FDs. Figure 6 displays the corresponding slope analysis when looking for a rise and drop in the TSI/UV respectively. We look for both kinds of extrema since both increases (from flares) and decreases (from dark spots) can be expected. For a decrease in TSI we find a slope significant above the 99.999 % level while the slope in the UV, when looking for a rise, is insignificant when the unusual Halloween event (FD 1) is disregarded. For a rise in TSI and a drop in UV the slopes are significant, but the extrema get larger with decreasing FD strength making this correlation somewhat unphysical. For the UV data two of the FDs (number 4 and 12 on the list) had to be excluded due to a critical gap in the dataset.

Based on the above we conclude that there is no connection between changes in UV and the FD strength. On the other hand we find a clear signal in the TSI at about $\sim 1.5\,\mathrm{W\,m^{-2}}$ – a correlation also seen in Laken et al. (2011). We are, however, not aware of any mechanism that could cause such a change in TSI, which is unrelated to UV, to have an impact on aerosols and clouds one week later, although a mechanism, involving surface heating and resulting circulation changes cannot be ruled out completely (Meehl et al., 2009). A response in water vapour also fits with the observed delay in the response since water has an atmospheric lifetime of about 9 days.

4.5 Signal delay

The delay between the FDs and the response in cloud parameters is 6–9 days, consistent with other cloud data sets (Svensmark et al., 2009). Assuming that the change in ionization affects the aerosol nucleation, there are several stages to go through before a change would be expected to be seen in the cloud data. First the aerosols, which nucleate at about 1 nm, need to grow to CCN sizes (up to $\sim$100 nm). Aerosol growth rates of about $1\,\mathrm{nm\,h^{-1}}$ are not uncommon (Kulmala et al., 2004) which could explain several days of delay. Secondly the aerosols need to be activated to become cloud droplets and the clouds need to adjust to the new droplet concentration, e.g. through

Discussion Paper | Discussion Paper | Discussion Paper | Discussion Paper |

ACPD

12, 3595–3617, 2012

Effects of cosmic ray decreases on cloud microphysics

J. Svensmark et al.

rain-out in the case of fewer (and thus probably larger) cloud drops. A response time of about a week in total is therefore not unreasonable.

5 Conclusions

Summarizing the observed effects on clouds, there are three things to note: (1) the observed parameters change consistently with each other during a Forbush decrease as seen in Table 3. (2) The signal is significant above 2–3 σ for CF, ϵ, τ, and LWP and between 1–2 σ for R_{eff} and CCN, consistent with derived values. The significance of the observations is reinforced by principal component analysis at the 3.1 σ level. (3) There appears to exist a correlation between the magnitude of the FD event and its effect in all of the parameters except CCN, where we show that the signal is expected to be drowned out by the noise. Furthermore we do not see a correlation with changes in UV, and while the TSI seems to change according to FD strength a microphysical mechanism involving aerosols and clouds is unavailable. In combination the observed responses make an actual FD-induced change in cloud microphysics more probable, and therefore support the conclusions of the SBS paper, which point to an ion-enhanced cloud life-cycle mechanism.

Supplementary material related to this article is available online at: http://www.atmos-chem-phys-discuss.net/12/3595/2012/acpd-12-3595-2012-supplement.zip.

Acknowledgements. We thank Henrik Spliid for valuable discussions regarding the statistics and Nigel Calder for helpful comments. We acknowledge receipt of the unpublished TSI data from the VIRGO Experiment on the cooperative ESA/NASA Mission SOHO (version d41_61_0803) from PMOD/WRC, Davos, Switzerland. We acknowledge Tom Woods (CU LASP), Gary Rottman (CU LASP), and Giuliana de Toma (NCAR, HAO) for the SOLSTICE data and Mark Weber (U. Bremen, Germany) for the GOME data. MODIS data were obtained from http://modis.gsfc.nasa.gov. MBE thanks the Carlsberg Foundation for financial support.

ACPD
12, 3595–3617, 2012

Effects of cosmic ray decreases on cloud microphysics

J. Svensmark et al.

References

Bagó, E. P. and Butler, C. J.: The influence of cosmic rays on terrestrial clouds and global warming, Astron. Geophys., 41, 4.18–4.22, 2000. 3596

Bondo, T., Enghoff, M. B., and Svensmark, H.: Model of optical response of marine aerosols to Forbush decreases, Atmos. Chem. Phys., 10, 2765–2776, doi:10.5194/acp-10-2765-2010, 2010. 3597

Calogovic, J., Albert, C., Arnold, F., Beer, J., Desorgher, L., and Flueckiger, E. O.: Sudden cosmic ray decreases: No change of global cloud cover, Geophys. Res. Lett., 37, L03802, doi:10.1029/2009GL041327, 2010. 3597, 3600

Dickinson, R. E.: Solar variability and the lower atmosphere, B. Am. Meteorol. Soc., 56, 1240–1248, 1975. 3596

Dragić, A., Aničin, I., Banjanac, R., Udovičić, V., Joković, D., Maletić, D., and Puzović, J.: Forbush decreases – clouds relation in the neutron monitor era, Astrophys. Space Sci. Trans., 7, 315–318, doi:10.5194/astra-7-315-2011, 2011. 3597

Forbush, S.: A model for particle formation and growth in the atmosphere with molecular resolution in size, Phys. Rev., 51, 1108, doi:10.1103/PhysRev.51.1108.3, 1937. 3596

Froehlich, C.: Solar irradiance variability since 1978 – Revision of the PMOD composite during solar cycle 21, Space Sci. Rev., 125, 53–65, doi:10.1007/s11214-006-9046-5, iSSI Workshop on Solar Variability and Planetary Climates, Bern, Switzerland, 6–10 June 2005, 2006. 3604

Hobbs, P. V.: Aerosol-Cloud-Climate Interactions, Academic Press, Inc., 1993. 3601

King, M. D., Tsay, S.-C., Platnick, S. E., Wang, M., and Liou, K.-N.: Cloud Retrieval Algorithms for MODIS: Optical Thickness, Effective Particle Radius, and Thermodynamic Phase, Tech. rep., 1997. 3603

Kristjánsson, J. E., Stjern, C. W., Stordal, F., Fjæraa, A. M., Myhre, G., and Jónasson, K.: Cosmic rays, cloud condensation nuclei and clouds – a reassessment using MODIS data, Atmos. Chem. Phys., 8, 7373–7387, doi:10.5194/acp-8-7373-2008, 2008. 3597, 3600

Kulmala, M., Vehkamäki, H., Petäjä, T., Dal Maso, M., Lauri, A., Kerminin, V. M., Birmili, W., and McMurry, P. H.: Formation and growth rates of ultrafine atmospheric particles: a review of observations, J. Aerosol Sci., 35, 143–176, 2004. 3596, 3604

Laken, B., Wolfendale, A., and Kniveton, D.: Cosmic ray decreases and changes in the liquid water cloud fraction over the oceans, Geophys. Res. Lett., 36, L23803,

ACPD

12, 3595–3617, 2012

Effects of cosmic ray decreases on cloud microphysics

J. Svensmark et al.

doi:10.1029/2009GL040961, 2009. 3597, 3601
Laken, B., Kniveton, D., and Wolfendale, A.: Forbush decreases, solar irradiance variations, and anomalous cloud changes, J. Geophys. Res., 116, D09201, doi:10.1029/2010JD014900, 2011. 3604
Levy, R. C., Remer, L. A., Kleidman, R. G., Mattoo, S., Ichoku, C., Kahn, R., and Eck, T. F.: Global evaluation of the Collection 5 MODIS dark-target aerosol products over land, Atmos. Chem. Phys., 10, 10399–10420, doi:10.5194/acp-10-10399-2010, 2010. 3598
Manninen, H. E., Nieminen, T., Asmi, E., Gagné, S., Häkkinen, S., Lehtipalo, K., Aalto, P., Vana, M., Mirme, A., Mirme, S., Hõrrak, U., Plass-Dülmer, C., Stange, G., Kiss, G., Hoffer, A., Törő, N., Moerman, M., Henzing, B., de Leeuw, G., Brinkenberg, M., Kouvarakis, G. N., Bougiatioti, A., Mihalopoulos, N., O'Dowd, C., Ceburnis, D., Arneth, A., Svenningsson, B., Swietlicki, E., Tarozzi, L., Decesari, S., Facchini, M. C., Birmili, W., Sonntag, A., Wiedensohler, A., Boulon, J., Sellegri, K., Laj, P., Gysel, M., Bukowiecki, N., Weingartner, E., Wehrle, G., Laaksonen, A., Hamed, A., Joutsensaari, J., Petäjä, T., Kerminen, V.-M., and Kulmala, M.: EUCAARI ion spectrometer measurements at 12 European sites – analysis of new particle formation events, Atmos. Chem. Phys., 10, 7907–7927, doi:10.5194/acp-10-7907-2010, 2010. 3597
Marsh, N. D. and Svensmark, H.: Low Cloud Properties Influenced by Cosmic Rays, Phys. Rev. Lett., 85, 5004–5007, doi:10.1103/PhysRevLett.85.5004, 2000. 3596, 3598
Meehl, G. A., Arblaster, J. M., Matthes, K., Sassi, F., and van Loon, H.: Amplifying the Pacific Climate Sytstem Response to a Small 11-Year Solar Cycle Forcing, Science, 325, 1114–1118, 2009. 3604
Miller, J. and Miller, J.: Statistics and Chemometrics for Analytical Chemistry, 4th edn., Prentice Hall, 2000. 3603
Remer, L., Kaufman, Y., Tanre, D., Mattoo, S., Chu, D., Martins, J., Li, R., Ichoku, C., Levy, R., Kleidman, R., Eck, T., Vermote, E., and Holben, B.: The MODIS aerosol algorithm, products, and validation, J. Atmos. Sci., 62, 947–973, doi:10.1175/JAS3385.1, 2005. 3598
Rohs, S., Spang, R., Rohrer, F., Schiller, C., and Vos, H.: A correlation study of high-altitude and midaltitude clouds and galactic cosmic rays by MIPAS-Envisat, J. Geophys. Res.-Atmos., 115, D14212, doi:10.1029/2009JD012608, 2010. 3597
Sloan, T. and Wolfendale, A. W.: Testing the proposed causal link between cosmic rays and cloud cover, Environ. Res. Lett., 3, 024001, doi:10.1088/1748-9326/3/2/024001, 2008. 3597, 3600
Snow-Kropla, E. J., Pierce, J. R., Westervelt, D. M., and Trivitayanurak, W.: Cosmic rays,

aerosol formation and cloud-condensation nuclei: sensitivities to model uncertainties, Atmos. Chem. Phys., 11, 4001–4013, doi:10.5194/acp-11-4001-2011, 2011. 3597

Stephens, G. L.: Radiation Profiles in Extended Water Clouds. II: Parameterization Schemes, J. Atmos. Sci., 35, 2123–2132, 1978. 3601

Svensmark, H. and Friis-Christensen, E.: Variation of cosmic ray flux and global cloud coverage – a missing link in solar-climate relationships, J. Atmos. Solar-Terr. Phy., 59, 1225–1232, doi:10.1016/S1364-6826(97)00001-1, 1997. 3596

Svensmark, H., Bondo, T., and Svensmark, J.: Cosmic ray decreases affect atmospheric aerosols and clouds, Geophys. Res. Lett., 36, L15101, doi:10.1029/2009GL038429, 2009. 3596, 3598, 3604

Todd, M. C. and Kniveton, D. R.: Short-term variability in satellite-derived cloud cover and galactic cosmic rays: an update, J. Atmos. Terr. Phys., 66, 1205–1211, 2004. 3597

Viereck, R. A. and Puga, L. C.: The NOAA Mg II core-to-wing solar index: Construction of a 20-year time series of chromospheric variability from multiple satellites, J. Geophys. Res., 104, 9995–10005, 1999. 3604

Woods, T., Eparvier, F., Fontenla, J., Harder, J., Kopp, G., McClintock, W., Rottman, G., Smiley, B., and Snow, M.: Solar irradiance variability during the October 2003 solar storm period, Geophys. Res. Lett., 31, L10802, doi:10.1029/2004GL019571, 2004. 3600

Yu, F. and Turco, R. P.: The size-dependent charge fraction of sub-3-nm particles as a key diagnostic of competitive nucleation mechanisms under atmospheric conditions, Atmos. Chem. Phys., 11, 9451–9463, doi:10.5194/acp-11-9451-2011, 2011. 3597

ACPD

12, 3595–3617, 2012

Effects of cosmic ray decreases on cloud microphysics

J. Svensmark et al.

Table 1. Thirteen FDs ranked according to their depression of ionization in the lower atmosphere. The events displayed meet the criteria of giving a reduction of more than 7 % in the South Pole neutron monitor, and being within the MODIS data range between years 2000 and 2006. The decrease is set relative to the overall change in ionization during the course of an 11-yr solar cycle such that an FD with a decrease of 100 % changes ionization as much as going from solar maximum to solar minimum does.

Order	Date	Decrease (%)
1	31 October 2003	119
2	19 January 2005	83
3	13 September 2005	75
4	16 July 2000	70
5	12 April 2001	64
6	10 November 2004	53
7	26 September 2001	50
8	17 July 2005	47
9	27 July 2004	45
10	31 May 2003	44
11	25 November 2001	39
12	15 May 2005	38
13	28 August 2001	37

ACPD
12, 3595–3617, 2012

Table 2. Parameters and their equivalents in the "MOD08_D3" data product.

Parameter	MODIS "MOD08_D3" parameter name
ϵ	Cloud_Effective_Emissivity_Mean
CCN	Cloud_Condensation_Nuclei_Ocean_Mean
τ	Cloud_Optical_Thickness_Liquid_Mean
LWP	Cloud_Water_Path_Liquid_Mean
CF	Cloud_Fraction_Liquid_Mean
R_{eff}	Cloud_Effective_Radius_Liquid_Mean

ACPD
12, 3595–3617, 2012

Effects of cosmic ray decreases on cloud microphysics

J. Svensmark et al.

Table 3. List of quantities calculated from FDs 1 to 5. The table shows both base level, percentage change $c_{P_{1..5,\mathrm{meas}}}$, derived change $c_{P_{1..5,\mathrm{der}}}$ estimated from Eqs. (1), (2), and (3) (the number in brackets refers to which equation was used), absolute change to noise ratio, and the day of the extremum of each parameter. The extremum days for each value differ from those in Fig. 1 (and the text) since they are the averages of the 5 individual event extrema whereas the figure shows the average of the 5 events taken together.

Parameter	Base level $\pm\sigma$	$c_{P_{1..5,\mathrm{meas}}}$ (%)	$c_{P_{1..5,\mathrm{der}}}$ (%)	$c_{P_{1..5,\mathrm{meas}}}$ (σ)	Extremum (days)
ϵ	0.686 ± 0.003	-1.29	-1.65 ± 0.78 [1]	-3.37	7.7 ± 4.5
CCN ($10^8\,\mathrm{cm}^{-2}$)	2.60 ± 0.06	-3.32	-2.49 ± 5.32 [3]	-1.35	6.1 ± 4.0
τ	11.09 ± 0.12	-2.87	-3.73 ± 1.54 [2]	-2.69	8.1 ± 4.5
LWP ($\mathrm{g\,m}^{-2}$)	108.60 ± 1.11	-3.05	-2.18 ± 1.61 [2]	-2.97	8.5 ± 4.1
CF	0.277 ± 0.004	-5.53	–	-4.03	9.5 ± 4.3
R_{eff} (µm)	16.95 ± 0.07	0.71	-0.19 ± 2.12 [2]	1.62	6.9 ± 4.3

ACPD
12, 3595–3617, 2012

Effects of cosmic ray decreases on cloud microphysics

J. Svensmark et al.

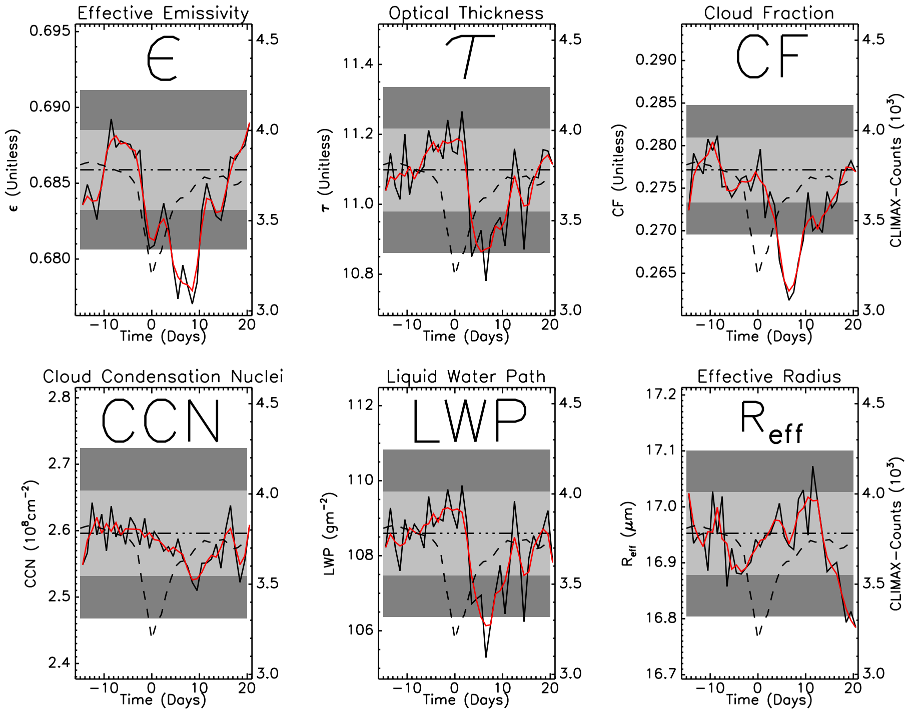

Fig. 1. Global daily means of the parameters ϵ, τ, CF, CCN, LWP, and R_{eff} averaged for Forbush decreases 1 to 5 (Table 1). The dashed line shows the averaged cosmic ray neutron counts from the Climax neutron monitor. The black curve is the response in the cloud parameter and the red curve shows a 3-day smoothed version of the black curve. The light and dark grey bands represent 1 and 2 σ centered around the base level (days −15 to −5).

ACPD
12, 3595–3617, 2012

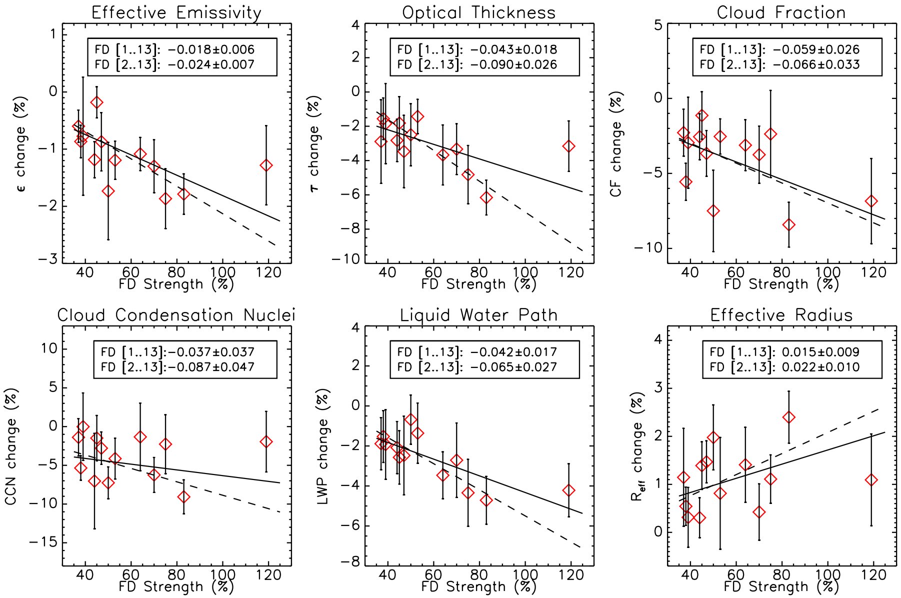

Fig. 2. Comparison of the Forbush decrease magnitude and its impact in each of the six parameters. Black lines indicate the weighted linear trends of the data points, with slope values and their standard deviation written on each plot. Broken lines indicate the linear trends with the exceptional 119 % Halloween Event (FD 1) excluded. Note that the x-axis starts at 30 %.

ACPD
12, 3595–3617, 2012

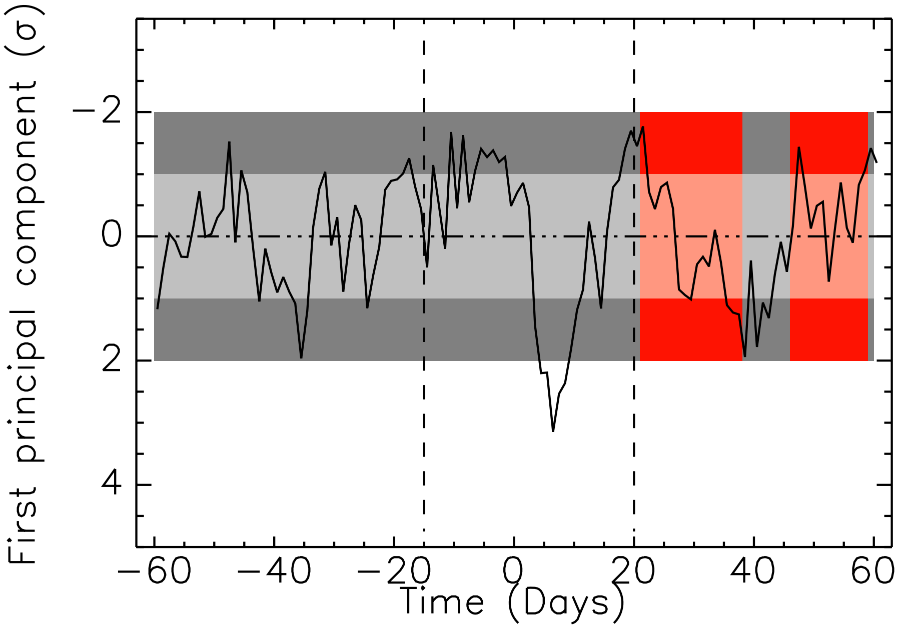

Fig. 3. The time series along the first principal component, obtained by averaging the 5 strongest events. The grey areas denote 1 and 2 standard deviations, respectively. The PC axis has been inverted. The red areas shows periods where missing data (or outliers) influence the averaging. The expression for PC1 is $-0.441 \cdot \epsilon - 0.502 \cdot \tau - 0.463 \cdot \mathrm{CF} - 0.232 \cdot \mathrm{CCN} - 0.470 \cdot \mathrm{LWP} + 0.255 \cdot R_{\mathrm{eff}}$. PC2 (not shown in the figure) is $0.313 \cdot \epsilon - 0.471 \cdot \tau + 0.400 \cdot \mathrm{CF} + 0.323 \cdot \mathrm{CCN} - 0.537 \cdot \mathrm{LWP} - 0.356 \cdot R_{\mathrm{eff}}$.

ACPD
12, 3595–3617, 2012

Effects of cosmic ray decreases on cloud microphysics

J. Svensmark et al.

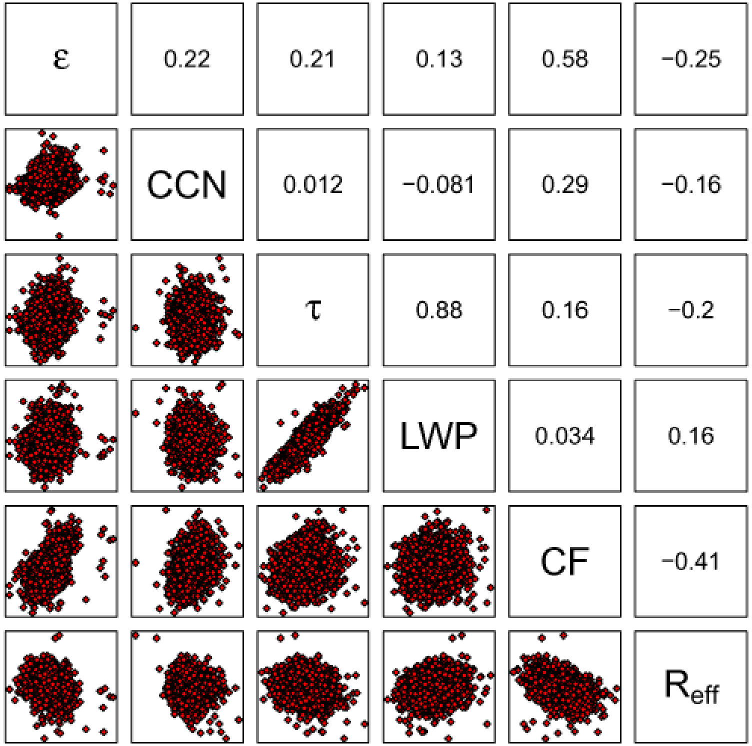

Fig. 4. Intercorrelation of the investigated parameters. Correlation plots are shown below the top-left to bottom-right diagonal, while the corresponding correlation coefficients are shown above. To prevent interference from singular data events all points exceeding 5 sigma have been removed from the data. Data was filtered for variations above 90 days using a Fourier filter, to remove seasonal variations.

ACPD
12, 3595–3617, 2012

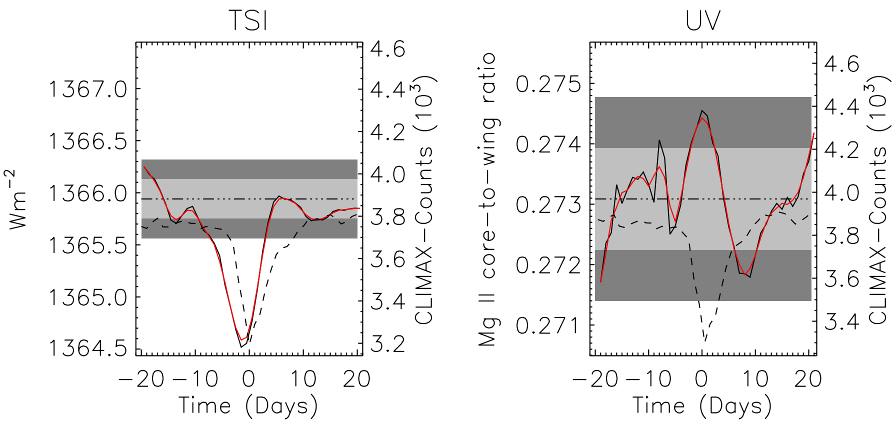

Fig. 5. Mean of the change in TSI (left) and UV (right) for the 5 largest Forbush decreases. The black curve is the signal, the red curve is the same data, using a 3-day smoothing. The dashed line is the neutron monitor count. Light and dark grey areas show 1 and 2 standard deviations, respectively.

ACPD
12, 3595–3617, 2012

Effects of cosmic ray decreases on cloud microphysics

J. Svensmark et al.

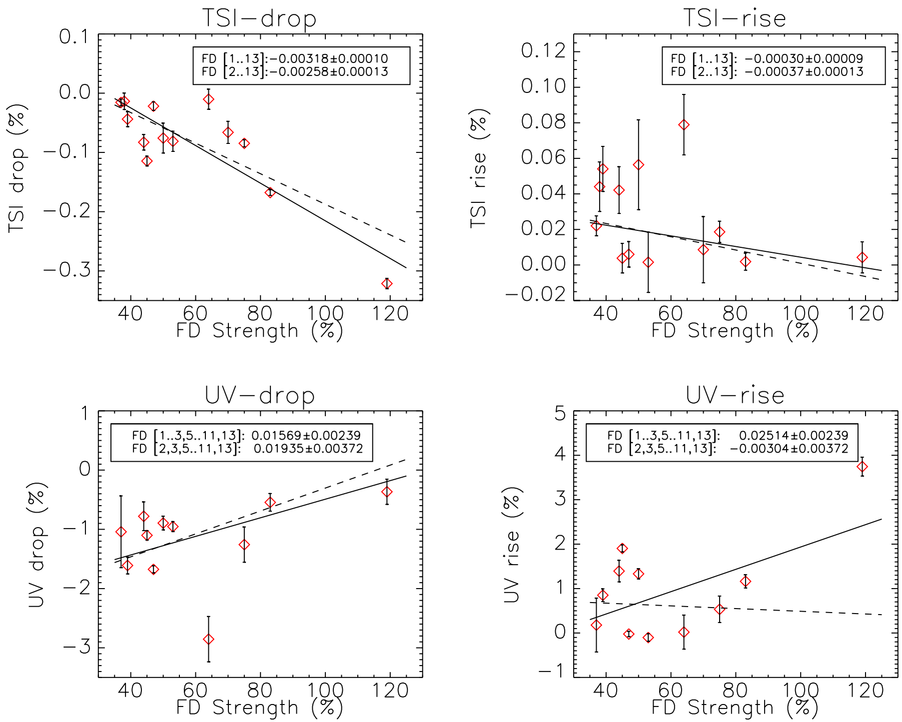

Fig. 6. Correlation between FD strength and change in TSI (top) and UV (bottom) when looking for a drop in signal (left) or a rise in signal (right). The broken line shows the trend when FD 1 is omitted.

ACPD
12, 3595–3617, 2012